Check for updates

Received: 24 March 2025 | Revised: 23 June 2025 | Accepted: 15 February 2026

DOI: 10.1002/npp2.70039

ORIGINAL PAPER

New Plant Protection Open Access WILEY

GameXPeptide synergistically enhances the control efficiency of *Metarhizium anisopliae* by inhibiting cotton aphid immunity

Xianfeng Yin[1,2] | **Xin Sun**[1] | **Fenglian Jia**[1] | **Shiqian Feng**[1] | **Rong Zhang**[3] | **Hidayat Ullah**[4] | **Fulian Wang**[2] | **Guangyue Li**[1] | **Xiongbing Tu**[1]

[1]State Key Laboratory for Biology of Plant Diseases and Insect Pests, Chinese Academy of Agricultural Sciences, Institute of Plant Protection, Beijing, China

[2]College of Agriculture, Yangtze University, Jingzhou, Hubei, China

[3]Ningxia Academy of Agriculture and Forestry Sciences, Institute of Plant Protection, Yinchuan, Ningxia, China

[4]Department of Agriculture, The University of Swabi, Swabi, Khyber Pakhtunkhwa, Pakistan

Correspondence

Fulian Wang, Guangyue Li and Xiongbing Tu.
Email: wangfl_hb@163.com, liguangyue@caas.cn and Xbtu@ippcaas.cn

Funding information

National Key R&D Program of Ningxia Hui Autonomous Region, Grant/Award Number: 2021BEF02006; Institute of Plant Protection, Chinese Academy of Agricultural Sciences, Grant/Award Number: CAAS-CSCB-202401

Abstract

The entomopathogenic fungus *Metarhizium anisopliae* plays a crucial role in sustainable agriculture by controlling diverse pests, but insect innate immunity hinders its efficacy by impeding spore germination. GameXPeptide (GXP), a metabolite derived from entomopathogenic nematode symbiotic bacteria, suppresses insect immunity, yet its interaction with entomopathogenic fungi (EPF) remained unstudied. This study demonstrates that GXP enhances the efficacy of *M. anisopliae* against cotton aphids, as evidenced by laboratory bioassays, metabolomic profiling, and experimental investigations. Our results reveal that GXP does not have any adverse effects on the fungus. However, the combined application of GXP and *M. anisopliae* significantly increases the mortality rate of cotton aphids. Furthermore, our findings indicate that this synergistic interaction notably influences the metabolic processes of cotton aphids. Notably, there is a significant decrease in purine metabolism compared to that in aphids infected solely by *M. anisopliae*. This alteration in purine metabolism could potentially account for the observed reduction in melanization in aphids infected by the fungus in the presence of GXP. In summary, our results highlight that the combined effect of GXP and *M. anisopliae* enhances the virulence of the fungus against cotton aphids by modulating their metabolism and immune responses. This study is the first to demonstrate that GXP can enhance the virulence of *M. anisopliae* against cotton aphids. These findings provide a novel strategy for improving biopesticide efficacy in sustainable agriculture.

KEYWORDS

cotton aphid, GXP, hypoxanthine, L-DOPA, melanization, *Metarhizium anisopliae*

1 | INTRODUCTION

The cotton aphid (*Aphis gossypii* Glover, Homoptera: Aphididae) causes serious damage to melons and cotton by sap sucking, transmitting viruses, and promoting the growth of sooty mold.[1] The main method of managing cotton aphids is the application of insecticides; however, *A. gossypii* is difficult to control due to its high reproductive capability and short generation cycle, which quickly lead to the development of resistance to many

Xianfeng Yin and Xin Sun contributed equally to this study.

This is an open access article under the terms of the Creative Commons Attribution License, which permits use, distribution and reproduction in any medium, provided the original work is properly cited.

© 2026 The Author(s). *New Plant Protection* published by John Wiley & Sons Australia, Ltd on behalf of Institute of Plant Protection, Chinese Academy of Agricultural Sciences.

chemical insecticides.[2] Moreover, chemical pesticides can have long-lasting negative effects on ecosystems[3,4] and human health,[4] highlighting the need to reduce their usage.

Alternatively, biopesticides offer a reliable way to protect plants. Entomopathogenic fungi (EPF) have been found to be effective biopesticides, with 750 EPF species available for controlling insect pests. One commonly used EPF is *Metarhizium anisopliae* (Metsch), which is effective against over 200 insect species, including *A. gossypii*.[5,6] To date, many strains of *M. anisopliae* have been commercialized.[7,8] However, the proportion of biopesticides used in practical applications remains limited. The main reason is that insects possess strong immune defenses, rendering biopesticides slower and less efficient as control agents. Recently, research has shown that bacteria produce compounds that enhance fungal infection of insects by disrupting host immunity or generating insecticidal toxins, thereby accelerating mortality.[9–11] Moreover, studies have found that synergistic interactions between biopesticides and other compounds can shorten pest kill time and increase mortality rates,[6,12,13] making this a promising approach for pest control.

GameXPeptides (GXPs), a class of cyclic pentapeptides, are common secondary metabolites produced by *Xenorhabdus* and *Photorhabdus*.[14] There are several different types of GXPs, including GXP-A, GXP-B, GXP-C, and GXP-D,[15] with GXP-A typically being the most abundant.[10] It has been proven that GXPs can effectively inhibit cellular immunity in insects.[16] For example, GXP-A has been applied to enhance the insecticidal activity of *Bacillus thuringiensis* against the lepidopteran insect *Spodoptera exigua*.[17] Despite evidence suggesting that GXP can enhance bacterial biopesticides, its compatibility with fungal agents such as *M. anisopliae* has not yet been investigated.

The insect immune system includes interconnected humoral and cellular defenses.[18] Humoral immunity involves recognizing pathogens in the hemolymph, activating protease cascades, generating antimicrobial peptides, and producing melanization intermediates and other immune factors in the blood-like hemolymph. Unlike fully metamorphic insects, aphids rely more heavily on the Jun N-terminal kinase (JNK) pathway to initiate melanization and cellular immune responses, as aphids lack many genes necessary for detecting pathogens.[19,20] Melanin, a key product of the melanization process, fights invaders by adhering to their surfaces, stabilizing wound clots,[21] and reinforcing the outer shells of insects.[22] Many enzymes and raw materials affect the formation of melanin, with one key enzyme being pivotal to its production. Phenoloxidase (PO), a key enzyme in melanin biosynthesis, is derived from the inactive zymogen prophenoloxidase (PPO) and is activated by aphids in response to pathogen infection.[20] Tyrosine hydroxylase (TH) catalyzes the hydroxylation of L-tyrosine (L-Tyr) to L-3,4-dihydroxyphenylalanine (L-DOPA),[23] and PO catalyzes the oxidation of L-DOPA into dopaquinone, which serves as a precursor to melanin formation.[24] The cellular immune response in insects is mediated by hemocytes, which can phagocytose and encapsulate pathogens.[25] When immune cells recognize pathogenic microorganisms, they secrete proinflammatory factors such as tumor necrosis factor (TNF-α) and interleukins (IL-1α, IL-1β, IL-6). These cytokines mobilize more immune cells and promote xanthine oxidase (XO) to metabolize insulin into uric acid, releasing reactive oxygen species (ROS: O_2- and H_2O_2) and nitrogen free radicals to eliminate pathogenic microorganisms.[26,27] Among these cytokines, IL-1α and IL-1β bind to and activate the same receptor,[28] promoting the release of other cytokines such as TNF-α and IL-6 and inducing Th17 expression in the adaptive immune response.[29] Some studies have reported that IL-6 and TNF-α can enhance the phagocytic activity of blood cells.[30,31] Although GXP has been reported to inhibit cellular immunity in insects,[16] its effect on the immune response of cotton aphids remains unclear.

This study aimed to improve the effectiveness of *M. anisopliae* in controlling plant pests by assessing its compatibility with different concentrations of GXP. Firstly, laboratory experiments were conducted to determine the optimal concentrations of GXP and *M. anisopliae*, from which the best combination was selected for subsequent field efficacy trials. Next, non-targeted metabolomics was employed to compare the differences in insect metabolites between the treatment with *M. anisopliae* combined with GXP and individual treatments during the infection process. The results showed that L-DOPA was significantly upregulated in the GXP treatment group compared to the control group without GXP, whereas hypoxanthine (HX) was downregulated. To verify whether the upregulation of L-DOPA affects the melanization reaction mediated by PO, the melanization reaction and PO activity in the hemolymph of cotton aphids were measured. Finally, the effect of HX on immune-related factors in the hemolymph of cotton aphids was studied to elucidate its role in the insect's innate defense system. This study reveals the mechanism by which GXP inhibits insect immunity and provides a novel method for controlling cotton aphids.

2 | MATERIALS AND METHODS

2.1 | Chemical reagents and biological materials

GXP used in this study was obtained from Professor Guangyue Li (IPP, CAAS). *A. gossypii* Glover was

29949890, 2026, 1, Downloaded from https://onlinelibrary.wiley.com/doi/10.1002/npp2.70039 by CochraneChina, Wiley Online Library on [08/06/2026]. See the Terms and Conditions (https://onlinelibrary.wiley.com/terms-and-conditions) on Wiley Online Library for rules of use; OA articles are governed by the applicable Creative Commons License

initially collected from a cotton field in Langfang (39.54°N, 116.70°E), Hebei Province, China, and subsequently reared on cotton plants (Lumian No. 1) grown in an artificial climate chamber under controlled conditions of 24 ± 1°C, 70% ± 5% relative humidity, and a 16:8-h light/dark cycle. The insects were maintained in the laboratory without exposure to any pathogenic microorganisms or insecticides. To identify aphids, molecular confirmation was performed. To obtain the full-length sequence (1563 bp) of the mitochondrial *COI* gene, two pairs of specific primers were designed to amplify two segments of mtDNA *COI* via polymerase chain reaction (PCR). One portion of mtDNA *COI* (783 bp) was amplified by PCR using the forward primer P1 and the reverse primer P2, and the other portion of mtDNA *COI* (805 bp) was amplified by PCR using the forward primer P3 and reverse primer P4.[16] The primers are listed in Supporting Information S1: Table S1.

The strain *M. anisopliae* IMI330189, isolated from *Locusta migratoria* and deposited in our laboratory (IPP, CAAS), was cultured on potato dextrose agar containing 5% yeast extract (PDAY) at 25°C for 8 days in an incubator. The spores were collected and suspended in sterilized distilled water containing 0.05% Tween-80. The concentration of the conidial suspension was determined using a hemocytometer. *M. anisopliae* was identified by molecular biology using the primers ITS1 and ITS4.

2.2 | Sampling and measurements

2.2.1 | Bioassays in laboratory

Four different final concentrations of GXP were utilized in this experiment. GXP was initially dissolved in dimethyl sulfoxide to achieve a concentration of 1 mg/mL and then diluted with 0.01% Tween-80 to obtain the corresponding final concentrations of 1.25, 2.5, 5, and 10 ng/mL. A blank control was also included, which included neither GXP nor fungus. Treatment with *M. anisopliae* at a final concentration of 2×10^8 spores/mL or GXP at a final concentration of 10 ng/mL was used as the positive control. The toxicity test was conducted using the immersion method. Uniform cotton leaflets were selected, and 30 cotton aphids were placed on each leaflet. The leaflets with aphids were fully submerged in the treatment solutions for 5 s and then removed and allowed to drain for 30 s to eliminate excess liquid. Afterward, the petioles of the cotton leaves were inserted into sterilized feeding devices containing 15 mL of 3% agar (Supporting Information S1: Figure S1). After sealing, the leaflets were placed in an artificial climate chamber maintained at 24°C. The number of aphid deaths was recorded on the third and fourth days. Each treatment consisted of four replicates ($n = 4$ replicates per treatment).

2.2.2 | Field efficacy experiment

The field efficacy experiment was conducted in June 2023 at the Juhua Tai Garden Farm (105.93°E, 37.08°N) in the Xixia District, Yinchuan City, Ningxia Hui Autonomous Region, China. A total of five treatments were established for this experiment: Treatment 1, water control (CK); Treatment 2, broflanilide (novel insecticide targeting aphid nerves, causing paralysis and death, and suppressing reproduction); Treatment 3, *M. anisopliae* (Ma); Treatment 4, GXP; and Treatment 5, *M. anisopliae* + GXP (Ma + GXP). Control plots (CK) received water with 0.01% Tween-80, which served as the solvent control for the other treatments. The reagent dosages for each treatment are shown in Supporting Information S1: Table S2. Fungal spores were present at a concentration of 2×10^8 spores/mL, GXP was prepared at 10 ng/mL, and broflanilide was used after a 1:1500 dilution. Each treatment had four plots, with each plot measuring 18 m^2 (3 m × 6 m, including six goji berry trees *Lycium barbarum*), resulting in a total of 20 plots covering 360 m^2. The plots were randomized using a block design to minimize environmental variability. A multifunctional electric backpack sprayer (3WBD-20L) was used for foliar spraying. To prevent pesticide drift during application, protective rows were set between each treatment. No pesticides were used during the experiment.

In each plot, three goji berry trees were randomly surveyed using the 5-point sampling method, in which one branch was selected from the east, south, west, north, and center of the tree for the fixed-point investigation (marked with a marker card). The total number of cotton aphids within a 30-cm range at the top of each branch was recorded before treatment (1 day) and after treatment (3, 7, and 14 days). The reduction rate of the pest population and the control effect were calculated using the following formulas:

$$\text{Reduced rate of pests} = \frac{(\text{No.of live individuals before treatment} - \text{No.of live individuals after treatment})}{\text{No.of live individuals before treatment}} \times 100\%$$

29949890, 2026, 1, Downloaded from https://onlinelibrary.wiley.com/doi/10.1002/npp2.70039 by CochraneChina, Wiley Online Library on [08/06/2026]. See the Terms and Conditions (https://onlinelibrary.wiley.com/terms-and-conditions) on Wiley Online Library for rules of use; OA articles are governed by the applicable Creative Commons License

$$\text{Control effect} = \frac{(\text{Reduction rate in the treatment area} - \text{Reduction rate in the control area})}{(1 - \text{Reduction rate in the control area})} \times 100\%$$

2.2.3 | Metabolomics analysis of cotton aphids

Metabolomics analysis of cotton aphids was conducted using the same sampling method as the bioassay in the laboratory. Cotton aphids treated with *M. anisopliae* (2×10^8 spores/mL) (Ma) and a mixture of *M. anisopliae* (2×10^8 spores/mL) and GXP (10 ng/mL) (Ma + GXP) for 3 days were used for metabolomics detection. Each treatment included four replicates, with 0.2 g of cotton aphids collected per replicate in a 1.5-mL centrifuge tube. The samples were quickly frozen in liquid nitrogen for 15 min and then stored at −80°C for subsequent testing.

2.2.4 | Expression of immune-related genes

cDNAs were synthesized with aphid RNAs from four treatments (same with metabolome assay) using FastKing gDNA Dispelling RT Super Mix (TIANGEN) according to the manufacturer's protocols. qRT-PCR was performed using Taq Pro Universal SYBR qPCR Master Mix (Q712-02, Vazyme) and the QuantStudio 6 Pro (Thermo Fisher Scientific). The PCR was conducted under the following conditions: 95°C for 30 s, followed by 40 cycles of 95°C for 10 s and 60°C for 30 s. At the end of each PCR run, a melting curve was generated from 65°C to 95°C, increasing by 0.5°C per 5 s, to ensure the specificity of the amplicon. All experiments were repeated three times. To determine the effect of GXP on the melanization reaction of the cotton aphid, we measured the transcriptional expression levels of *melanization protease 1 (MP1)*, which encodes a serine protease acting as a key activator in the PPO cascade. Primers MP1-F and MP1-R were designed using SnapGene 8.0 (https://support.snapgene.com/). *Elongation factor 1 alpha (EF1α)* was used as the internal control with the following pairs of primers: EF1α-F and EF1α-R.[20]

2.2.5 | Determination of melanization reaction in the hemolymph of cotton aphids

The treatment of the test insects followed the same method as the metabolomics test, with samples collected 72 h after treatment. Hemolymph extraction was performed with slight modifications to a previously described method.[32] Aphids were washed with sterilized water, disinfected with 75% ethanol, and then placed on ice. A 1.5-mL centrifuge tube was prepared by placing a sterilized plastic sheet (8 mm wide and 2.5 cm long, folded into a Z shape) at the bottom, with cotton wool spread on top of the sheet. The head of each cotton aphid was carefully removed with dissecting scissors, and the remaining body was placed into the prepared 1.5 mL centrifuge tube on ice. The tubes were then centrifuged at 4°C and 10,000 g for 15 min to extract the hemolymph of cotton aphids. One hundred cotton aphids from each treatment group were collected for melanization reaction detection. After hemolymph extraction, 4 μL of hemolymph from each treatment group was transferred into a PCR tube and promptly mixed with 6 μL of phosphate-buffered saline (PBS). The mixture was gently stirred, left at room temperature, and photographed and recorded after 80 min.

2.2.6 | Determination of PO activity in the hemolymph of cotton aphids

The effect of *M. anisopliae* combined with GXP on phenol oxidase activity in the hemolymph of cotton aphids was assessed. The treatment method for the test insects was the same as that used for metabolomics analysis. For each treatment, the sample size of cotton aphids was 160. After extracting the hemolymph, 4 μL of hemolymph from each treatment was mixed with 6 μL of PBS and placed on ice for immediate use in the experiment. A diluted hemolymph sample of 2 μL was added to a 96-well plate, followed by the addition of 98 μL of 2 mM L-DOPA solution, with three technical replicates. The samples were incubated in a full-function microplate reader at 37°C for 30 min. After shaking for 5 s, the absorbance value was measured at 490 nm.

The standard curve was determined using the Bradford protein assay.[33] The 1-mg/mL standard was prepared by dissolving 0.01 g of bovine serum albumin and 0.08766 g of NaCl in water, with the volume made up to 10 mL. A series of standards diluted with 0.15 M NaCl to final concentrations of 0.1, 0.2, 0.4, 0.6, and 0.8 mg/mL were prepared. Then, 90 μL of pre-prepared dye solution (0.05 g G-250, 23.75 mL anhydrous ethanol, 42.5 mL phosphoric acid, adjusted to a total

29949890, 2026, 1, Downloaded from https://onlinelibrary.wiley.com/doi/10.1002/npp2.70039 by CochraneChina, Wiley Online Library on [08/06/2026]. See the Terms and Conditions (https://onlinelibrary.wiley.com/terms-and-conditions) on Wiley Online Library for rules of use; OA articles are governed by the applicable Creative Commons License

volume of 500 mL) was mixed with 10 μL of the diluted sample (2.5-fold dilution) or the standard sample. The mixture was then added to a 96-well plate, and the absorbance was measured at 595 nm. The standard curve was plotted, and the concentration of the sample was calculated based on the standard curve.

2.2.7 | Effect of HX on hemocytes in cotton aphids

To determine the effect of HX on the phagocytic activity of hemocytes in cotton aphids, we first measured the activities of IL-1β, IL-6, and TNF-α. Hemolymph was extracted as described above. A 200-μL drop of Grace's insect medium was placed on a clean, precooled Petri dish and covered with a lid. Sixty decapitated cotton aphids from each treatment group were introduced into the precooled medium. After centrifugation at 350 g for 15 s, the supernatant was collected. The supernatant was then centrifuged again at 350 g for an additional 10 min. The sediment was retained, and the cells were resuspended in Grace's insect medium to obtain the hemocyte dilution required for the experiment.

To verify that HX can activate blood cells, XO and allopurinol (ALL) were preincubated for 4 h (to allow for full reaction) before the addition of blood cells. A total of four treatments were set up for the research experiment: Treatment 1 (control, CK), Treatment 2 (HX), Treatment 3 (HX + XO), and Treatment 4 (HX + XO + ALL). The specific concentrations for each treatment are shown in Supporting Information S1: Table S3. In each treatment, 100 μL of blood cell dilution was added and incubated at 28°C for 5 h. Afterward, after centrifugation at 350 g at 4°C for 10 min, the supernatant was collected, and the levels of IL-1β, IL-6, and TNF-α were measured according to the instructions of the reagent kits. All operations were performed under aseptic conditions.

Later, we measured the effect of HX on the phagocytic activity of cotton aphid hemocytes. The hemocytes of the cotton aphid were extracted according to the procedure outlined above. Hemocytes were incubated with HX (200 μM) at 28°C for 30 min, then 0.1% neutral red was added and further incubated for 6 h. Afterward, centrifugation was performed at 350 g for 5 min, the supernatant was discarded, and 200 μL of lysis solution (acetic acid/anhydrous ethanol = 1:1) was added and placed in a refrigerator at 4°C for 12 h. Finally, the absorbance value was measured using a fully automated microplate reader (SpectraMax M3), with three replicates for each treatment.

2.3 | Data analysis

The two-way analysis of variance (ANOVA) was conducted using the *F*-test via the Anova function in the car package, followed by Tukey's honest significant difference test. All data were analyzed using R version 4.4.2 (https://www.r-project.org/, accessed on 31 October 2024). Graphs were plotted using GraphPad Prism version 9.0 (https://www.graphpad.com). The significance threshold was set at $p < 0.05$, and the highly significant threshold was set at $p < 0.01$.

3 | RESULTS

3.1 | GXP enhances the virulence of *M. anisopliae* against the cotton aphid

GXPs are cyclic pentapeptides produced by *Xenorhabdus* and *Photorhabdus*[14] that can suppress insect cellular immunity and enhance the efficacy of bacterial biopesticides.[16] In this study, we combined GXP with *M. anisopliae* to investigate whether GXPs can improve the insecticidal performance of fungal agents. Firstly, we tested the effects of different concentrations of GXP on the spore germination and colony growth of *M. anisopliae*. Except for the highest concentration (100 ng/mL), no significant differences were found compared to the control group (CK) (Figure 1).

Furthermore, bioassays were conducted to investigate the effects of Ma and GXP on aphids. At 3 and 4 days post-application, the lethality of the Ma or GXP single-treatment groups did not differ significantly from that of the CK group. However, the combined treatment of Ma + GXP (2.5, 5, and 10 ng/mL) resulted in significantly higher aphid lethality compared to that of the CK group, with the lowest concentration of GXP (1.25 ng/mL) in the combined treatment showing no significant effect. Moreover, the lethality of the combined treatment of Ma + GXP (10 ng/mL) was significantly higher than that of the Ma or GXP single-treatment groups, except for 5 ng/mL. These findings indicate that the combination of *M. anisopliae* (10 ng/mL) with GXP (10 ng/mL) provides the most effective synergistic control of the cotton aphid (Figure 2A,B).

To further evaluate whether the optimal combination identified in the laboratory was also effective under field conditions, we tested the efficacy of *M. anisopliae* (2×10^8 spores/mL) combined with GXP (10 ng/mL) against cotton aphids using a spray method. At Day 3 post-application, both the Ma and Ma + GXP treatments showed significantly higher reduction rates of pests and control efficacy compared to the blank control and GXP alone. However, both were significantly lower than those of the broflanilide treatment (Figure 2C,D). Meanwhile, both the pest population reduction rate and control efficacy of the combined treatment of Ma + GXP were significantly higher than those of the Ma treatment at this time point. By Day 7, the population reduction

29949890, 2026, 1, Downloaded from https://onlinelibrary.wiley.com/doi/10.1002/npp2.70039 by CochraneChina, Wiley Online Library on [08/06/2026]. See the Terms and Conditions (https://onlinelibrary.wiley.com/terms-and-conditions) on Wiley Online Library for rules of use; OA articles are governed by the applicable Creative Commons License

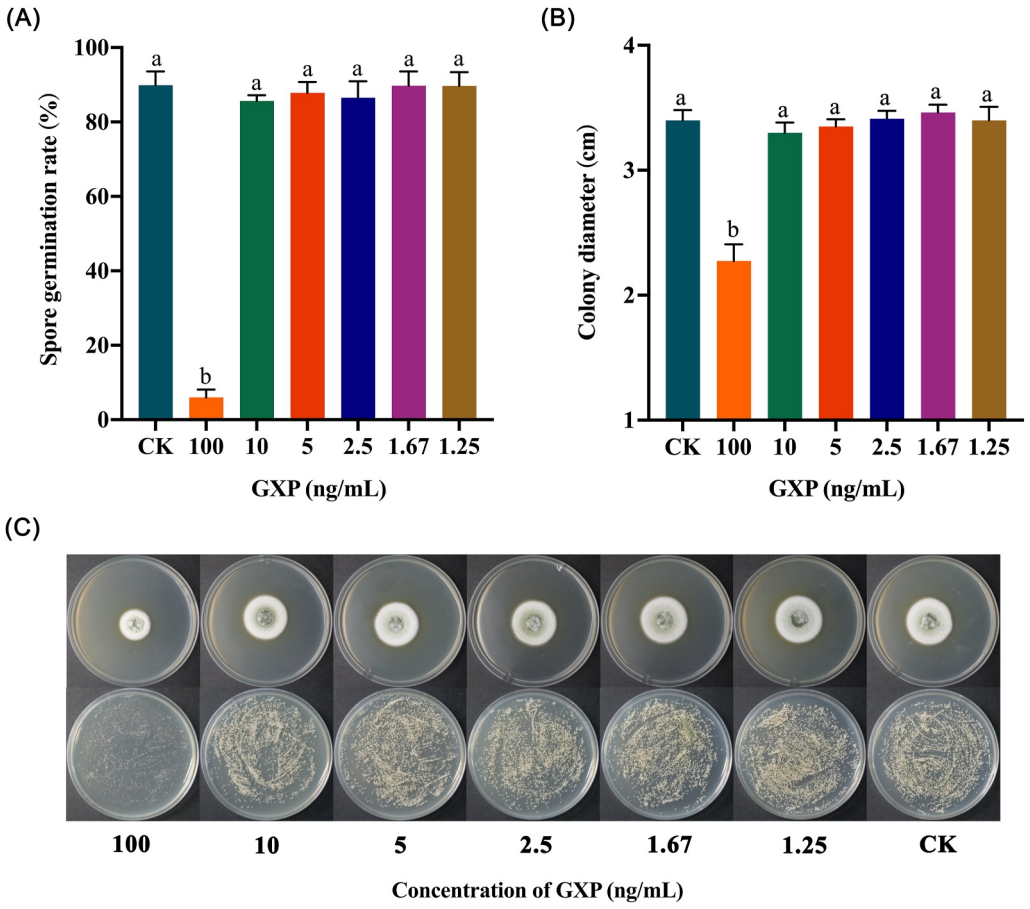

FIGURE 1 Effect of different concentrations of GXP on the germination and growth rate of *Metarhizium anisopliae*. The effects of different concentrations (100, 10, 5, 2.5, 1.67, and 1.25 ng/mL) of GXP on the spore germination rate (A), the colony diameter (B), and the growth (top row) and spore germination (bottom row) of *M. anisopliae* (C). CK was inoculated with 0.01% Tween-80. Data in the figure are presented as mean ± SD. Different lowercase letters indicate significant differences between treatments, as determined by Duncan's test ($p < 0.01$). The *M. anisopliae* conidial suspension was adjusted to a final concentration of approximately 2×10^6 spores/mL in 0.01% Tween-80. Spores were considered germinated when the length of the germ tube equaled the width of the spore. A 20-μL sample of each GXP concentration was added to a 90-mm PDAY plate. Sterilized circular filter paper (7 mm in diameter) saturated with 20 μL of conidial suspension (approximately 2×10^6 spores/mL) was placed in the center of the plate and cultured at 28°C for 8 days. GXP, GameXPeptide.

rate and control efficacy of the Ma + GXP group were significantly higher than those of the Ma group, and both of these groups were obviously superior to those of the broflanilide treatment (Figure 2C,D). A similar trend of control efficacy persisted through the later observations at Day 14 (Figure 2D), which indicates the long-lasting effectiveness of Ma.

3.2 | Differential metabolomics between treatments with *M. anisopliae* and a mixture of *M. anisopliae* and GXP

The principal component analysis of the metabolites from cotton aphids after treatment with Ma, GXP, and Ma + GXP showed that the samples predominantly fell within the 95% confidence intervals. The CK group was distinctly separated from the other treatments. However, the groups corresponding to different treatments were relatively close to each other, as observed by the inability to separate GXP from Ma + GXP (Figure 3A,B and Supporting Information S1: Figure S2). A total of 122 differential metabolites were identified between the Ma and Ma + GXP treatments, meeting the criteria of $p < 0.05$, variable importance in projection >1, and |fold change| > 2 (Figure 3C,D). Among them, 77 metabolites were detected in electrospray ionization negative mode (ESI−) and 45 in electrospray ionization positive mode (ESI+). Compared with the Ma treatment alone, 28 ESI− metabolites were upregulated and 49 were downregulated, whereas 22 ESI+ metabolites were upregulated and 23 were downregulated.

Among these differential metabolites, we identified 2 substances directly involved in the melanization and cellular immunity of cotton aphids (Figure 3E).

29949890, 2026, 1, Downloaded from https://onlinelibrary.wiley.com/doi/10.1002/npp2.70039 by CochraneChina, Wiley Online Library on [08/06/2026]. See the Terms and Conditions (https://onlinelibrary.wiley.com/terms-and-conditions) on Wiley Online Library for rules of use; OA articles are governed by the applicable Creative Commons License

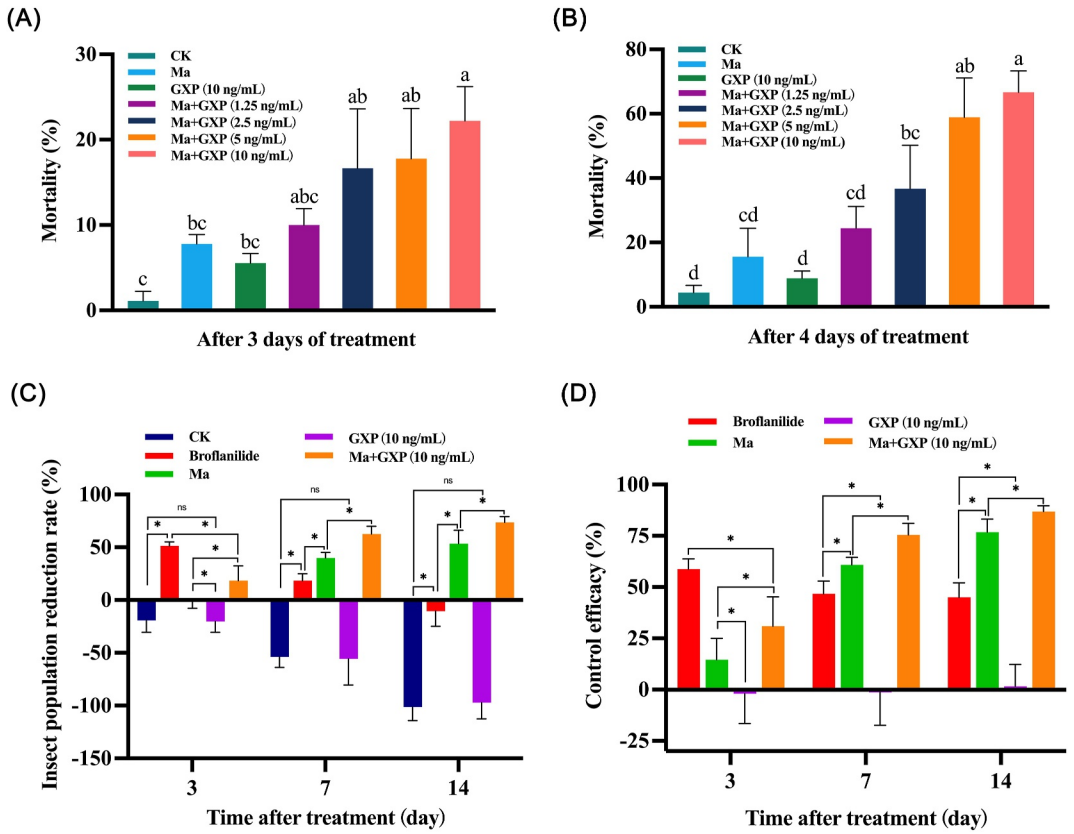

FIGURE 2 The combined toxicity of *Metarhizium anisopliae* (Ma) and different concentrations of GXP was measured on cotton aphids in the laboratory (A, B) using the immersion method and in the field (C, D) through efficacy experiments. The data presented in the figure are shown as mean ± SD. According to Duncan's test ($p < 0.05$), different lowercase letters indicate significant differences between treatments. The notation * represents significant differences at the level of $p < 0.05$ across different treatments. GXP, GameXPeptide.

Compared to the group without GXP treatment (CK and Ma), the relative expression of *MP2835* (*HX*) in the GXP-treated group (GXP and Ma + GXP) was significantly downregulated, whereas the opposite trend was observed for the relative expression of *MP5815* (*L-DOPA*). HX serves as a purine precursor necessary for nucleic acid synthesis, supporting hemocyte proliferation and activation during cellular immune responses. The downregulation of *HX* suggests impaired purine metabolism, which is critical for hemocyte proliferation, thereby suppressing cellular immunity. L-DOPA, a key precursor in the melanization pathway of insects, is derived from tyrosine through the action of TH and is further oxidized by PO into dopamine quinone. The relative expression of L-DOPA was significantly increased in the GXP-treated group, which means that the synthesis of the substance was not affected. Given that PO can be activated by MP1, we further measured the relative expression of the *MP1* gene. Compared with the blank control (CK), *MP1* expression was significantly downregulated in the Ma, GXP, and Ma + GXP treatment groups ($p < 0.05$). Moreover, the Ma + GXP group showed a significant reduction in *MP1* expression compared to the Ma group alone ($p < 0.05$; Figure 3F).

3.3 | Effect of L-DOPA on the melanization reaction

Because L-DOPA is a precursor for melanin synthesis in the melanization reaction, we aimed to verify whether the upregulation of L-DOPA directly affects the melanization reaction in cotton aphids. The melanization activity in cotton aphid hemolymph after treatment with Ma and Ma + GXP was detected in vitro. The results indicated that, compared to *M. anisopliae* alone, the melanization activity in the hemolymph of cotton aphids treated with Ma + GXP was inhibited (Figure 4A). This was inconsistent with the increased L-DOPA expression in the hemolymph observed with the mixed treatment in the metabolomics results (Figure 3E). It means that the expression of L-DOPA is not the limiting factor in the inhibition of cotton aphid immunity by GXP. We further determined PO activity and found that its expression in the Ma + GXP-treated group was significantly lower than that in the Ma treatment group (Figure 4B), which coincided with the significant reduction of *MP1* expression. This implies that the observed decrease in PO activity may lead to the accumulation of L-DOPA.

Previous research has found that the melanization reaction in insects is activated by PPO, which converts

29949890, 2026, 1, Downloaded from https://onlinelibrary.wiley.com/doi/10.1002/npp2.70039 by CochraneChina, Wiley Online Library on [08/06/2026]. See the Terms and Conditions (https://onlinelibrary.wiley.com/terms-and-conditions) on Wiley Online Library for rules of use; OA articles are governed by the applicable Creative Commons License

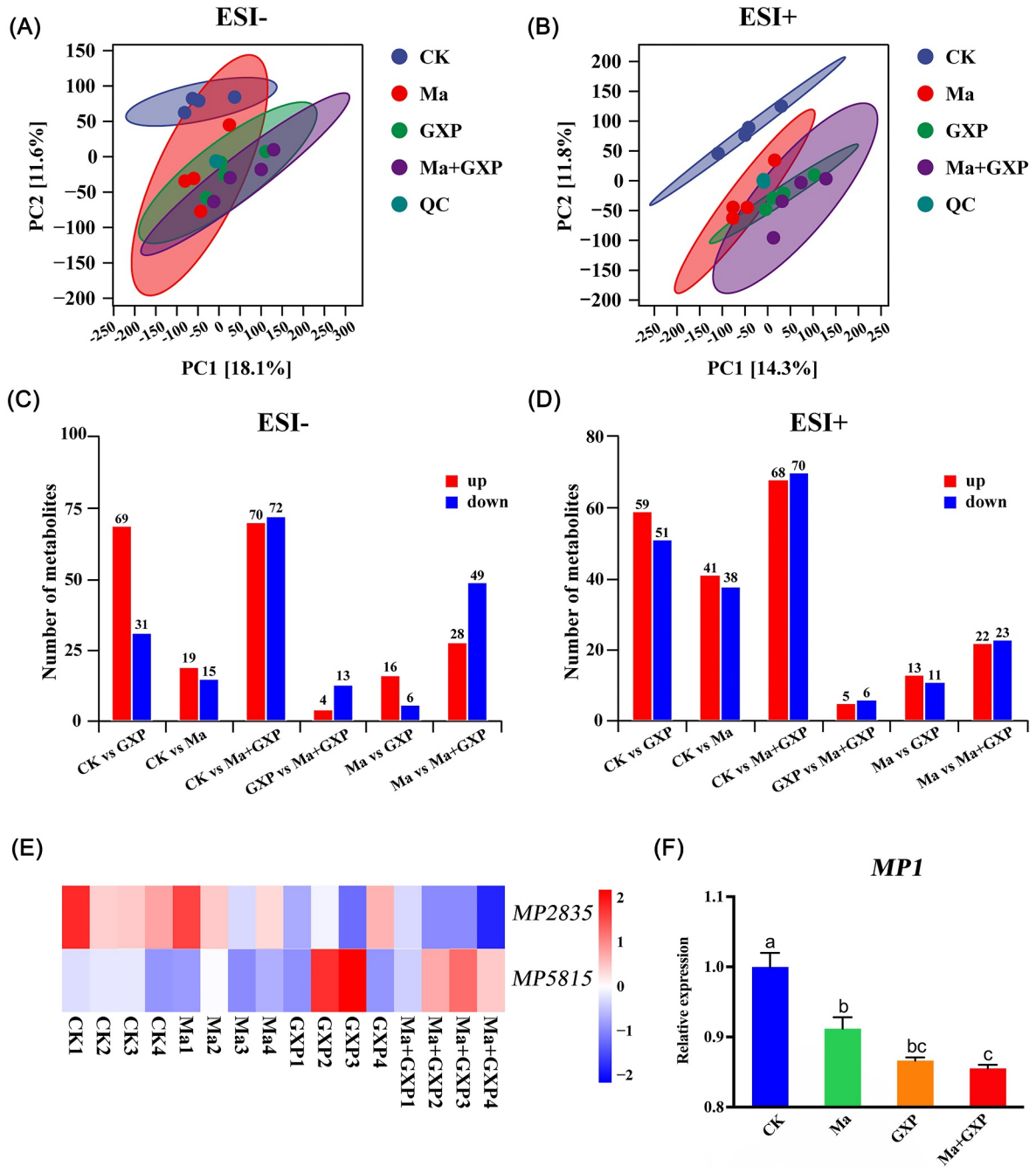

FIGURE 3 The effects of treatments with *Metarhizium anisopliae* and GXP on the metabolites and gene expression in *Aphis gossypii*. (A) PCA in the ESI− scan mode revealed that the first two components explained 18.1% and 11.6% of the variance, respectively. (B) In the ESI+ scan mode, cotton aphids subjected to the same treatment combinations showed that the first two components accounted for 14.3% and 11.8% of the variance, respectively. Each point represents a sample, with the distance between points indicating the similarity between samples. The identified differential metabolites are shown in a bar chart in the ESI− mode (C) and the ESI+ mode (D). (E) Differential metabolic substances related to melanization and cellular immunity in cotton aphids. (F) The relative expression of the *MP1* gene. Different letters labeled above the columns mean a difference level of $p < 0.05$ after one-way ANOVA analysis. ANOVA, analysis of variance; ESI+, electrospray ionization positive mode; ESI−, electrospray ionization negative mode; GXP, GameXPeptide; MP1, melanization protease 1; PCA, principal component analysis.

tyrosine to Dopa, followed by its oxidation to dopachrome, dihydroxyindole, and finally melanin.[34] The PO and melanization activities were significantly inhibited in cotton aphids after treatment with GXP. Therefore, we propose that GXP may inhibit the conversion of L-DOPA to dopaquinone by suppressing PO activity in cotton aphids, ultimately inhibiting the melanization reaction.

29949890, 2026, 1, Downloaded from https://onlinelibrary.wiley.com/doi/10.1002/npp2.70039 by CochraneChina, Wiley Online Library on [08/06/2026]. See the Terms and Conditions (https://onlinelibrary.wiley.com/terms-and-conditions) on Wiley Online Library for rules of use; OA articles are governed by the applicable Creative Commons License

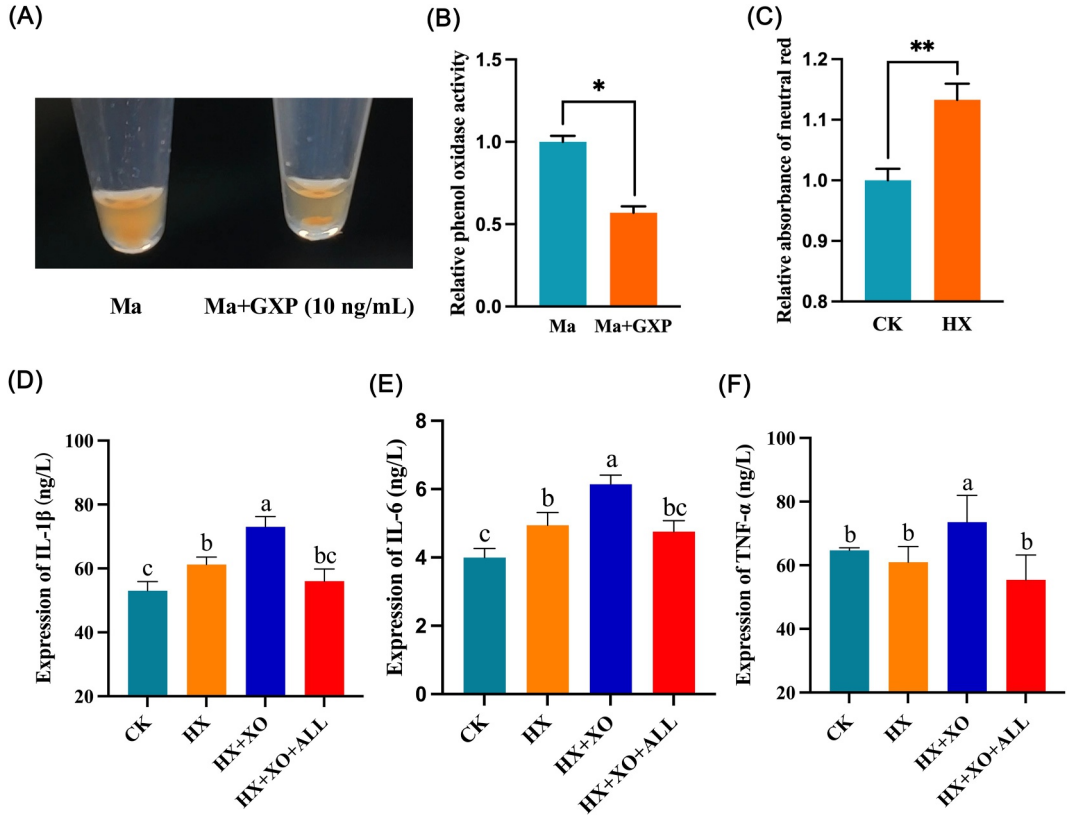

FIGURE 4 Results of various immune-related indices in cotton aphids: (A) Effects of *Metarhizium anisopliae* and Ma + GXP on the hemolymph melanization response. (B) The relative expression of PO due to Ma and Ma + GXP in cotton aphids. (C) The relative phagocytic activity of blood cells on neutrophils after treatment with HX. The expression of IL-1β (D), IL-6 (E), and TNF-α (F) secreted by blood cells of cotton aphids treated with HX, XO, and ALL. The data in the figure are presented as mean ± SE. ALL, allopurinol; CK, control; GXP, GameXPeptide; HX, hypoxanthine; PO, phenoloxidase; XO, xanthine oxidase. The notations "*" and "**" represent significant differences ($p < 0.05$ and $p < 0.001$) among different treatments, respectively.

3.4 | Impact of HX on the phagocytic activity of hemocytes in cotton aphids, with a specific focus on IL-1β, IL-6, and TNF-α levels

To evaluate the potential of HX in promoting blood cell activity, we quantified the phagocytic activity after HX treatment. The relative absorbance of neutral red after incubation with HX was significantly higher ($p < 0.001$) compared to the control group (CK; Figure 4C), which indicates that HX can enhance the phagocytic activity of hemocytes.

To further investigate the function of HX, XO and ALL were used. XO can metabolize HX to xanthine, which is subsequently converted to uric acid, with contemporary production of ROS. ALL is a specific XO inhibitor. We analyzed the secretion of immune factors in the treatment groups of HX, HX + XO, and HX + XO + ALL. Compared with the control group, HX treatment significantly increased the secretion of IL-1β and IL-6 ($p < 0.05$), whereas TNF-α showed no significant change (Figure 4D–F). When hemocytes were exposed to the HX + XO mixture, the secretion levels of IL-1β, IL-6, and TNF-α all increased significantly compared to HX treatment alone ($p < 0.05$). However, in the HX + XO + ALL group, the secretion levels of all three cytokines did not differ significantly from those in the control or HX groups ($p > 0.05$) (Figure 4D–F). These results indicate that HX plays a role in promoting hemocytes to secrete IL-1β, IL-6, and TNF-α (Figure 4D–F).

4 | DISCUSSION

In recent years, the extensive use of chemical pesticides has led to increasingly severe insecticide resistance in cotton aphids. *M. anisopliae*, an entomopathogenic fungus with broad-spectrum insecticidal activity and a low risk of inducing insect resistance, exhibits slow action and inconsistent efficacy. These limitations are largely attributed to the robust immune defense systems of insects, which inhibit fungal infection. GXP, a cyclic peptide metabolite derived from symbiotic bacteria of entomopathogenic nematodes, effectively suppresses hemocyte diffusion and nodulation reactions in insects. Recent studies have shown that GXP can inhibit insect

29949890, 2026, 1, Downloaded from https://onlinelibrary.wiley.com/doi/10.1002/npp2.70039 by CochraneChina, Wiley Online Library on [08/06/2026]. See the Terms and Conditions (https://onlinelibrary.wiley.com/terms-and-conditions) on Wiley Online Library for rules of use; OA articles are governed by the applicable Creative Commons License

immune responses and enhance the insecticidal activity of biopesticides.[10,17] However, the interaction between GXP and EPF remains uninvestigated. This paper employs laboratory and field virulence assays, along with molecular experiments at the humoral and cellular immune levels, to elucidate the joint action mechanism between GXP and *M. anisopliae*.

We evaluated the compatibility of *M. anisopliae* with different concentrations of GXP, as well as their virulence against cotton aphids. The optimal combination identified for controlling cotton aphids was Ma + GXP (10 ng/ml), resulting in an indoor mortality of 66.67% against cotton aphids 4 days post-treatment (Figure 2A). Field efficacy trials utilizing this optimal combination demonstrated control efficacy exceeding 60% on both Day 7 and Day 14 (Figure 2D). To further elucidate the synergistic mechanism of *M. anisopliae* and GXP, a nontargeted metabolomics analysis of cotton aphids was conducted. The metabolome results indicated that, except for CK, the differences among the metabolites of the other groups were not significant, and the number of distinct substances was limited (Figure 3A–D). However, among these distinct substances, we identified a significant upregulation of L-DOPA, which is related to the melanization reaction, and a downregulation of HX, which is associated with cellular immunity (Figure 3E). Interestingly, L-DOPA plays a crucial role in the melanization reaction in insects. The melanization reaction in aphids primarily relies on the JNK pathway for pathogen recognition and elicits immune responses through PO and hemocyte-mediated immune reactions.[20] PO, which is converted from the inactive zymogen PPO, influences melanization by catalyzing the conversion of L-DOPA to dopaquinone, which is further transformed into melanin. We also determined the expression level of the *MP1* gene that activates PO and its enzyme activity. We found that the expression level of *MP1* and the activity of the PO enzyme in the Ma + GXP group were significantly lower than those in the Ma group (Figures 3F and 4B). This implies that the conversion of L-DOPA to dopaquinone is blocked, leading to the accumulation of L-DOPA, which is consistent with the metabolome results (Figure 3E). Meanwhile, we also determined the melanization reaction in the hemolymph of cotton aphids under Ma + GXP and Ma treatments, which showed that melanin levels in the Ma + GXP group were significantly lower than those in the Ma group. These findings align with the downregulation of *MP1* gene expression and reduced PO activity.

HX is oxidized to uric acid by XO, generating ROS.[26] This process activates nuclear factor-kappa B (NF-κB) and enhances the production of immune factors such as TNF-α. Previous studies suggest that uric

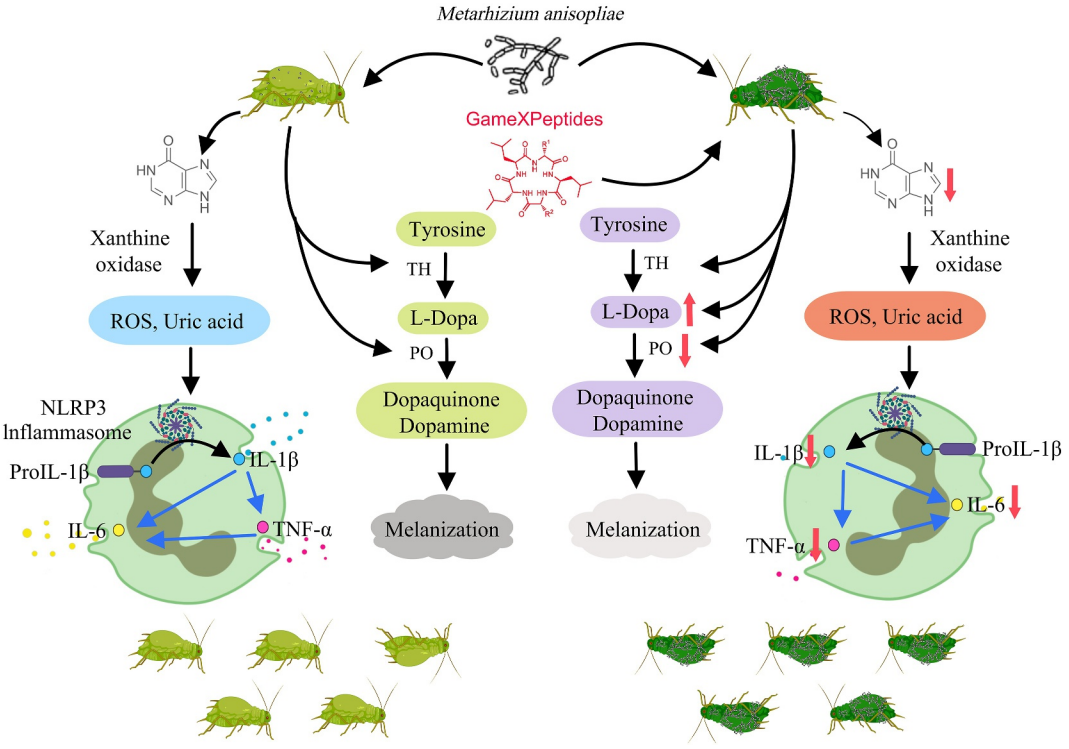

FIGURE 5 The effect of GXP on the melanization and cellular immunity of *Aphis gossypii* when subjected to *Metarhizium anisopliae*. After GXP treatment, the decreased PO activity in *A. gossypii* resulted in a weakened melanization reaction. Additionally, the decreased HX content led to a reduction in cytokines (IL-1β, IL-6, and TNF-α), which subsequently lowered the phagocytic activity of hemocytes. GXP, GameXPeptide; HX, hypoxanthine; IL, interleukins; PO, phenoloxidase; ROS, reactive oxygen species; TH, tyrosine hydroxylase; TNF, tumor necrosis factor.

29949890, 2026, 1, Downloaded from https://onlinelibrary.wiley.com/doi/10.1002/npp2.70039 by CochraneChina, Wiley Online Library on [08/06/2026]. See the Terms and Conditions (https://onlinelibrary.wiley.com/terms-and-conditions) on Wiley Online Library for rules of use; OA articles are governed by the applicable Creative Commons License

acid can stimulate the activity of blood cells, activate the NALP3 inflammasome, enhance antigen-specific immune responses, boost immunity, and reduce the risk of infection. Uric acid can also activate the NALP3 inflammasome in mice,[35] promoting the release of the immune factor IL-1β,[30] and it can further promote the secretion of IL-1β and IL-6 by vascular epithelial cells.[36] Our findings showed that HX promotes the phagocytic activity of hemocytes in cotton aphids (Figure 4C). We found that HX significantly promotes the release of IL-1β and IL-6 (Figure 4D,E), whereas TNF-α was not significantly affected (Figure 4F). However, the release of IL-1β, IL-6, and TNF-α was significantly enhanced when both HX and XO were present. Immune factors such as IL-6 and IL-1β can promote the phagocytic activity of blood cells,[37] further recruiting more immune cells and releasing reactive oxygen and nitrogen free radicals to eliminate pathogenic microorganisms. Ives et al. stated that XO converts HX to xanthine and then to uric acid, with ROS produced as a byproduct during this process.[38] More importantly, ROS is crucial for the activation of the NLRP3 inflammasome and the subsequent secretion of IL-1β. This conclusion is highly consistent with the expression trend of IL-1β in the experimental system of this study, which further confirms the reliability of this metabolism-inflammation regulatory mechanism. Meanwhile, the results for TNF-α in this study are consistent with the trend reported by Marraccini et al.[26] Meanwhile, Liu et al. demonstrated that inhibiting XO activity with ALL in *Mycobacterium tuberculosis* (MTB)-infected macrophages not only reduced the production of ROS and suppressed the activation of the NF-κB signaling pathway but also significantly downregulated both the mRNA expression and protein secretion levels of the proinflammatory cytokines TNF-α, IL-1β, and IL-6.[39]

Therefore, we believe that GXP may cause metabolic disorders in the purine pathway of cotton aphids by inhibiting the production of HX, further suppressing the production of immune factors IL-1β, IL-6, and TNF-α, and reducing the phagocytic activity of hemocytes. This, in turn, affects the response of cotton aphid hemocytes to pathogens.

5 | CONCLUSION

Based on the findings presented, GXP serves as a potent synergist for *Metarhizium anisopliae* in controlling cotton aphids. Its synergistic effect is achieved through two key mechanisms: Firstly, it downregulates *MP1* expression, which inhibits PO activity, thereby suppressing melanization; secondly, it reduces HX levels, leading to a diminishment of hemocyte-mediated immunity (Figure 5). This study identifies GXP as a promising synergist for *M. anisopliae*, offering a sustainable alternative to chemical pesticides by enhancing fungal virulence through dual suppression of aphid immune pathways.

AUTHOR CONTRIBUTIONS

Xianfeng Yin: Conceptualization; investigation; funding acquisition; writing—original draft; methodology; validation; writing—review and editing; visualization; project administration; formal analysis; software; data curation; supervision; resources. **Xin Sun:** Conceptualization; investigation; funding acquisition; writing—original draft. **Fenglian Jia:** Investigation. **Shiqian Feng:** Methodology. **Rong Zhang:** Project administration. **Hidayat Ullah:** Software. **Fulian Wang:** Resources. **Guangyue Li:** Investigation. **Xiongbing Tu:** Investigation; visualization; validation; project administration.

ACKNOWLEDGMENTS

This work was financially supported by the National Key Research and Development Program of Ningxia Hui Autonomous Region (2021BEF02006), People's Republic of China, and the Innovation Program of Chinese Academy of Agricultural Sciences (CAAS-CSCB-202401).

CONFLICT OF INTEREST STATEMENT

The authors declare no conflicts of interest.

DATA AVAILABILITY STATEMENT

The data that support the findings of this study are available upon request from the corresponding author. The data are not publicly available due to privacy or ethical restrictions.

ORCID

Xianfeng Yin https://orcid.org/0009-0007-2350-7065
Xiongbing Tu https://orcid.org/0000-0003-0676-8777

REFERENCES

1. Leroy, P. D., Sabri, A., Heuskin, S., Thonart, P., Lognay, G., Verheggen, F. J., Francis, F., Brostaux, Y., Felton, G. W., & Haubruge, E. (2011). Microorganisms from aphid honeydew attract and enhance the efficacy of natural enemies. *Nature Communications*, *2*(1), 348. https://doi.org/10.1038/ncomms1347
2. Hao, M., Sun, Z., Xu, J., Lv, M., & Xu, H. (2020). Semisynthesis and pesticidal activities of derivatives of the diterpenoid andrographolide and investigation on the stress response of *Aphis citricola* Van der Goot (Homoptera: Aphididae). *Journal of Agricultural and Food Chemistry*, *68*(14), 4131–4143. https://doi.org/10.1021/acs.jafc.9b08242
3. Kaur, R., Choudhary, D., Bali, S., Bandral, S. S., Singh, V., Ahmad, M. A., Rani, N., Singh, T. G., & Chandrasekaran, B. (2024). Pesticides: An alarming detrimental to health and environment. *Science of the Total Environment*, *915*, 170113. https://doi.org/10.1016/j.scitotenv.2024.170113
4. Pathak, V. M., Verma, V. K., Rawat, B. S., Kaur, B., Babu, N., Sharma, A., Dewali, S., Yadav, M., Kumari, R., Singh, S., Mohapatra, A., Pandey, V., Rana, N., & Cunill, J. M. (2022). Current status of pesticide effects on environment, human

29949890, 2026, 1, Downloaded from https://onlinelibrary.wiley.com/doi/10.1002/npp2.70039 by CochraneChina, Wiley Online Library on [08/06/2026]. See the Terms and Conditions (https://onlinelibrary.wiley.com/terms-and-conditions) on Wiley Online Library for rules of use; OA articles are governed by the applicable Creative Commons License

health and it's eco-friendly management as bioremediation: A comprehensive review. *Frontiers in Microbiology*, *13*, 962619. https://doi.org/10.3389/fmicb.2022.962619

5. Jandricic, S. E., Filotas, M., Sanderson, J. P., & Wraight, S. P. (2014). Pathogenicity of conidia-based preparations of entomopathogenic fungi against the greenhouse Pest aphids *Myzus persicae, Aphis gossypii*, and *Aulacorthum solani* (Hemiptera: Aphididae). *Journal of Invertebrate Pathology*, *118*, 34–46. https://doi.org/10.1016/j.jip.2014.02.003
6. Nawaz, A., Razzaq, F., Razzaq, A., Gogi, M. D., Fernández-Grandon, G. M., Tayib, M., Ayub, M. A., Sufyan, M., Shahid, M. R., Qayyum, M. A., Naveed, M., Ijaz, A., & Arif, M. J. (2022). Compatibility and synergistic interactions of fungi, *Metarhizium anisopliae*, and insecticide combinations against the cotton aphid, *Aphis gossypii* glover (hemiptera: Aphididae). *Scientific Reports*, *12*(1), 4843. https://doi.org/10.1038/s41598-022-08841-6
7. Camargo, M. G., Marciano, A. F., Sá, F. A., Perinotto, W. M., Quinelato, S., Gôlo, P. S., Angelo, I. C., Prata, M. C., & Bittencourt, V. R. (2014). Commercial formulation of *Metarhizium anisopliae* for the control of *rhipicephalus microplus* in a pen study. *Veterinary Parasitology*, *205*(1–2), 271–276. https://doi.org/10.1016/j.vetpar.2014.07.011
8. Sullivan, C. F., Parker, B. L., & Skinner, M. (2022). A review of commercial *Metarhizium*-and *Beauveria*-based biopesticides for the biological control of ticks in the USA. *Insects*, *13*(3), 260. https://doi.org/10.3390/insects13030260
9. Wei, G., Lai, Y., Wang, G., Chen, H., Li, F., & Wang, S. (2017). Insect pathogenic fungus interacts with the gut microbiota to accelerate mosquito mortality. *Proceedings of the National Academy of Sciences of the United States of America*, *114*(23), 5994–5999. https://doi.org/10.1073/pnas.1703546114
10. Jin, G., Hrithik, M. T. H., Lee, D. H., Kim, I. H., Jung, J. S., Bode, H. B., & Kim, Y. (2023). Manipulation of GameXPeptide synthetase gene expression by a promoter exchange alters the virulence of an entomopathogenic bacterium, *Photorhabdus temperata temperata*, by modulating insect immune responses. *Frontiers in Microbiology*, *14*, 1271764. https://doi.org/10.3389/fmicb.2023.1271764
11. Henkel, J. S., Baldwin, M. R., & Barbieri, J. T. (2010). Toxins from bacteria. In A. Luch (Ed.), *Molecular, Clinical and Environmental Toxicology* (pp. 1–29). https://doi.org/10.1007/978-3-7643-8338-1_1
12. Bitsadze, N., Jaronski, S., Khasdan, V., Abashidze, E., Abashidze, M., Latchininsky, A., Samadashvili, D., Sokhadze, I., Rippa, M., Ishaaya, I., & Horowitz, A. R. (2013). Joint action of *Beauveria bassiana* and the insect growth regulators diflubenzuron and novaluron, on the migratory locust, *Locusta migratoria*. *Journal of Pest Science*, *86*(2), 293–300. https://doi.org/10.1007/s10340-012-0476-4
13. Rice, S. J., & Furlong, M. J. (2023). Synergistic interactions between three insecticides and *Beauveria bassiana* (Bals.-Criv.) Vuill. (ascomycota: Hypocreales) in lesser mealworm, *Alphitobius diaperinus* panzer (coleoptera: Tenebrionidae), larvae. *Journal of Invertebrate Pathology*, *200*, 107974. https://doi.org/10.1016/j.jip.2023.107974
14. Tobias, N. J., Wolff, H., Djahanschiri, B., Grundmann, F., Kronenwerth, M., Shi, Y. M., Simonyi, S., Grün, P., Shapiro-Ilan, D., Pidot, S. J., Stinear, T. P., Ebersberger, I., & Bode, H. B. (2017). Natural product diversity associated with the nematode symbionts *Photorhabdus* and *Xenorhabdus*. *Nature Microbiology*, *2*(12), 1676–1685. https://doi.org/10.1038/s41564-017-0039-9
15. Bode, H. B., Reimer, D., Fuchs, S. W., Kirchner, F., Dauth, C., Kegler, C., Lorenzen, W., Brachmann, A. O., & Grün, P. (2012). Determination of the absolute configuration of peptide natural products by using stable isotope labeling and mass spectrometry. *Chemistry (Weinheim an der Bergstrasse, Germany)*, *18*(8), 2342–2348. https://doi.org/10.1002/chem.201103479
16. Ffrench-Constant, R., Waterfield, N., Daborn, P., Joyce, S., Bennett, H., Au, C., Dowling, A., Boundy, S., Reynolds, S., & Clarke, D. (2003). *Photorhabdus*: Towards a functional genomic analysis of a symbiont and pathogen. *FEMS Microbiology Reviews*, *26*(5), 433–456. https://doi.org/10.1111/j.1574-6976.2003.tb00625.x
17. Hrithik, M. T. H., Park, Y., Park, H., & Kim, Y. (2022). Integrated biological control using a mixture of two entomopathogenic bacteria, *Bacillus thuringiensis* and *Xenorhabdus hominickii*, against *Spodoptera exigua* and other congeners. *Insects*, *13*(10), 860. https://doi.org/10.3390/insects13100860
18. Vilmos, P., & Kurucz, E. (1998). Insect immunity: Evolutionary roots of the mammalian innate immune system. *Immunology Letters*, *62*(2), 59–66. https://doi.org/10.1016/s0165-2478(98)00023-6
19. Gerardo, N. M., Altincicek, B., Anselme, C., Atamian, H., Barribeau, S. M., de Vos, M., Duncan, E. J., Evans, J. D., Gabaldón, T., Ghanim, M., Heddi, A., Kaloshian, I., Latorre, A., Moya, A., Nakabachi, A., Parker, B. J., Pérez-Brocal, V., Pignatelli, M., Rahbé, Y., … Vilcinskas, A. (2010). Immunity and other defenses in pea aphids, *Acyrthosiphon pisum*. *Genome Biology*, *11*(2), R21. https://doi.org/10.1186/gb-2010-11-2-r21
20. Ma, L., Liu, L., Zhao, Y., Yang, L., Chen, C., Li, Z., & Lu, Z. (2020). JNK pathway plays a key role in the immune system of the pea aphid and is regulated by microRNA-184. *PLoS Pathogens*, *16*(6), e1008627. https://doi.org/10.1371/journal.ppat.1008627
21. Eleftherianos, I., & Revenis, C. (2011). Role and importance of phenoloxidase in insect hemostasis. *Journal of Innate Immunity*, *3*(1), 28–33. https://doi.org/10.1159/000321931
22. Andersen, S. O. (2010). Insect cuticular sclerotization: A review. *Insect Biochemistry and Molecular Biology*, *40*(3), 166–178. https://doi.org/10.1016/j.ibmb.2009.10.007
23. Bueno-Carrasco, M. T., Cuéllar, J., Flydal, M. I., Santiago, C., Kråkenes, T. A., Kleppe, R., López-Blanco, J. R., Marcilla, M., Teigen, K., Alvira, S., Chacón, P., Martinez, A., & Valpuesta, J. M. (2022). Structural mechanism for tyrosine hydroxylase inhibition by dopamine and reactivation by Ser40 phosphorylation. *Nature Communications*, *13*(1), 74. https://doi.org/10.1038/s41467-021-27657-y
24. Vavricka, C., Han, Q., Huang, Y., Erickson, S. M., Harich, K., Christensen, B. M., & Li, J. (2011). From L-dopa to dihydroxyphenylacetaldehyde: A toxic biochemical pathway plays A vital physiological function in insects. *PLoS One*, *6*(1), e16124. https://doi.org/10.1371/journal.pone.0016124
25. Boman, H. G., & Hultmark, D. (1987). Cell-free immunity in insects. *Annual Review of Microbiology*, *41*(1), 103–126. https://doi.org/10.1146/annurev.mi.41.100187.000535
26. Marraccini, C., Merolle, L., Casali, E., Baricchi, R., & Pertinhez, T. A. (2022). Proof of concept: Hypoxanthine from stored red blood cells induces neutrophil activation. *Blood Transfusion*, *20*(2), 120–126. https://doi.org/10.2450/2020.0208-20
27. Mesquita Casagrande, A. C., Wamser, M. N., de Lima, D. D., Pereira da Cruz, J. G., Wyse, A. T., & Dal Magro, D. D. (2013). In vitro stimulation of oxidative stress by hypoxanthine in blood of rats: Prevention by vitamins E plus C and allopurinol. *Nucleotides and Nucleic Acids*, *32*(1), 42–57. https://doi.org/10.1080/15257770.2012.760043
28. Schneider, A., & Cohen-Solal, M. (1996). Hematologically important mutations: Triosephosphate isomerase. *Blood Cells, Molecules, and Diseases*, *22*(1), 82–84. https://doi.org/10.1006/bcmd.1996.0011
29. Chung, Y., Chang, S. H., Martinez, G. J., Yang, X. O., Nurieva, R., Kang, H. S., Ma, L., Watowich, S. S., Jetten, A. M., Tian, Q., & Dong, C. (2009). Critical regulation of early Th17 cell differentiation by interleukin-1 signaling. *Immunity*, *30*(4), 576–587. https://doi.org/10.1016/j.immuni.2009.02.007
30. Kumakura, S., Yamaguchi, Y., Murakawa, Y., & Kasukabe, T. (2018). Effect of cytokines and hyperthermia on phagocytosis

29949890, 2026, 1, Downloaded from https://onlinelibrary.wiley.com/doi/10.1002/npp2.70039 by CochraneChina, Wiley Online Library on [08/06/2026]. See the Terms and Conditions (https://onlinelibrary.wiley.com/terms-and-conditions) on Wiley Online Library for rules of use; OA articles are governed by the applicable Creative Commons License

and phosphatidylserine externalization: Implication for the pathophysiology of hemophagocytic syndrome. *Annals of Clinical and Laboratory Science*, *48*(3), 314–322.
31. Yang, S., Ma, Y., Lou, X., Zhou, Z., Zhang, H., Yi, S., Cheng, Y., Qian, S., Huang, M., & Fei, H. (2023). The role of TNF-α in the phagocytosis of largemouth bass (Micropterus salmoides) leukocytes. *Fish & Shellfish Immunology*, *132*, 108488. https://doi.org/10.1016/j.fsi.2022.108488
32. Schmitz, A., Anselme, C., Ravallec, M., Rebuf, C., Simon, J. C., Gatti, J. L., & Poirié, M. (2012). The cellular immune response of the pea aphid to foreign intrusion and symbiotic challenge. *PLoS One*, *7*(7), e42114. https://doi.org/10.1371/journal.pone.0042114
33. Ninfa, A. J., Ballou, D. P., & Benore, M. (2010). Response to review of fundamental laboratory approaches for biochemistry and biotechnology. *Biochemistry and Molecular Biology Education: A Bimonthly Publication of the International Union of Biochemistry and Molecular Biology*, *38*(2), 64. John Wiley and Sons. https://doi.org/10.1002/bmb.20383
34. Huang, C. Y., Christensen, B. M., & Chen, C. C. (2005). Role of dopachrome conversion enzyme in the melanization of filarial worms in mosquitoes. *Insect Molecular Biology*, *14*(6), 675–682. https://doi.org/10.1111/j.1365-2583.2005.00597.x
35. Mitra, S., & Abraham, E. (2006). Participation of superoxide in neutrophil activation and cytokine production. *Biochimica et Biophysica Acta*, *1762*(8), 732–741. https://doi.org/10.1016/j.bbadis.2006.06.011
36. Zhang, Y., Hong, Q., Huang, Z., Xue, P., Lv, Y., Fu, B., Chen, X., & Wu, D. (2014). ALDR enhanced endothelial injury in hyperuricemia screened using SILAC. *Cellular Physiology and Biochemistry*, *33*(2), 479–490. https://doi.org/10.1159/000358628
37. Han, P., Gong, Q., Fan, J., Abbas, M., Chen, D., & Zhang, J. (2022). Destruxin A inhibits scavenger receptor B mediated melanization in *Aphis citricola*. *Pest Management Science*, *78*(5), 1915–1924. https://doi.org/10.1002/ps.6809
38. Ives, A., Nomura, J., Martinon, F., Roger, T., LeRoy, D., Miner, J. N., Simon, G., Busso, N., & So, A. (2015). Xanthine oxidoreductase regulates macrophage IL1β secretion upon NLRP3 inflammasome activation. *Nature Communications*, *6*(1), 6555. https://doi.org/10.1038/ncomms7555
39. Liu, R., Zhang, F., Li, S., Liu, Q., Pang, Y., & Li, L. (2024). Regulation of ROS metabolism in macrophage via xanthine oxidase is associated with disease progression in pulmonary tuberculosis. *Metabolomics*, *20*(6), 127. https://doi.org/10.1007/s11306-024-02194-z

SUPPORTING INFORMATION

Additional supporting information can be found online in the Supporting Information section at the end of this article.

29949890, 2026, 1, Downloaded from https://onlinelibrary.wiley.com/doi/10.1002/npp2.70039 by CochraneChina, Wiley Online Library on [08/06/2026]. See the Terms and Conditions (https://onlinelibrary.wiley.com/terms-and-conditions) on Wiley Online Library for rules of use; OA articles are governed by the applicable Creative Commons License